NASA TECHNICAL NOTE

NASA TN D-6322

BUCKLING LOAD OF THIN CIRCULAR CYLINDRICAL SHELLS FORMED BY PLASTIC EXPANSION

by LeRoy R. Guist

Ames Research Center
Moffett Field, Calif. 94035

NATIONAL AERONAUTICS AND SPACE ADMINISTRATION • WASHINGTON, D. C. • APRIL 1971

1. Report No.	2. Government Accession No.	3. Recipient's Catalog No.
NASA TN D-6322		

4. Title and Subtitle	5. Report Date
BUCKLING LOAD OF THIN CIRCULAR CYLINDRICAL SHELLS FORMED BY PLASTIC EXPANSION	April 1971
	6. Performing Organization Code
7. Author(s)	8. Performing Organization Report No.
LeRoy R. Guist	A-3733
	10. Work Unit No.
9. Performing Organization Name and Address	124-08-14-10-00-21
Ames Research Center Moffett Field, California 94035	11. Contract or Grant No.
	13. Type of Report and Period Covered
12. Sponsoring Agency Name and Address	Technical note
National Aeronautics and Space Administration Washington, D. C. 20546	14. Sponsoring Agency Code

15. Supplementary Notes

16. Abstract

An experimental investigation was made to determine the axial buckling load of cylinders formed by a process of plastic expansion due to internal pressure. Test cylinders 21.6 cm in diameter, 0.330 mm thick, were formed by plastic expansion from 15.23 cm diameter commercial, welded, type 304 stainless steel tubing. Buckling loads from 50 to 71 percent of the classical value showed a definite relationship with the local decrease in curvature due to the worst imperfections. Buckling loads were substantially higher than expected in relation to the amplitude of their geometric imperfections.

The results indicate that the process of plastic expansion may provide a means of producing certain types of cylinders of unusually high buckling load at low cost.

17. Key Words (Suggested by Author(s))	18. Distribution Statement
Shells Cylindrical Cylindrical shell(s) Buckling Imperfection(s)	Unclassified -- Unlimited

19. Security Classif. (of this report)	20. Security Classif. (of this page)	21. No. of Pages	22. Price*
Unclassified	Unclassified	16	$3.00

*For sale by the Clearinghouse for Federal Scientific and Technical Information
Springfield, Virginia 22151

SYMBOLS

A	point midway between an inward imperfection peak and the prevous outward peak
B	point midway between an inward imperfection peak and the following outward peak
C_I	dimensionless parameter expressing local curvature reduction due to an inward geometric imperfection peak
E	modulus of elasticity
h_1, h_2	successive peak to peak imperfection amplitudes
P	experimental buckling load
P_{CL}	classical buckling load
$P_{(w)}$	buckling load predicted in reference 5 for a cylinder containing a flat spot imperfection of circumferential width w
R	mean radius of cylindrical shell
R_I	fictitious radius of curvature used in equation (2)
R_L	local radius of curvature at an inward imperfection peak
t	shell thickness
w	width of an inward imperfection peak
w_{CR}	critical width of a flat spot imperfection
δ	amplitude of an inward imperfection peak

BUCKLING LOAD OF THIN CIRCULAR CYLINDRICAL SHELLS FORMED BY PLASTIC EXPANSION

LeRoy R. Guist

Ames Research Center

SUMMARY

An experimental investigation was made to determine the axial buckling load of cylinders formed by a process of plastic expansion due to internal pressure. Test cylinders 21.6 cm in diameter, 0.330 mm thick, were formed by plastic expansion from 15.23 cm diameter commercial, welded, type 304 stainless steel tubing. Buckling loads from 50 to 71 percent of the classical value showed a definite relationship with the local decrease in curvature due to the worst imperfections. Buckling loads were substantially higher than expected in relation to the amplitude of their geometric imperfections.

The results indicate that the process of plastic expansion may provide a means of producing certain types of cylinders of unusually high buckling load at low cost.

INTRODUCTION

Theoretical and experimental work on the sensitivity to geometric imperfections of the buckling load of axially compressed cylinders has included studies of axially symmetric, random, and localized imperfections. These studies have resulted in considerable understanding of the effect of the geometry and amplitude of imperfections; but the problem of designing and manufacturing a cylindrical shell to sustain an axial compressive load closely approaching its classical value remains that of making a more perfect shell. Perfection, of course, requires great manufacturing precision and expense.

This study explores the possibilities of forming cylinders with a high degree of perfection by a relatively simple process of plastic expansion by means of internal pressure. A series of seven test cylinders, 21.6 cm diameter, 0.330 mm thick, 19 cm long, was formed by expansion under nearly pure hoop stress conditions from 15.23 cm diameter type 304 commercial welded stainless steel tubing. Geometric imperfections were measured in order to detect any characteristic imperfections resulting from the expansion process and to indicate any correlation between severity of imperfections and buckling load. With the exception of specimen 7, all test specimens were formed without deliberate imperfections. In the case of specimen 7, the precision outer form was modified in an attempt to produce a "flat spot" imperfection.

PREPARATION OF TEST SPECIMENS

Test specimens were formed from commercially available 15.23 cm diameter type 304 welded stainless steel tubing by hydrostatic expansion. A length of tubing sealed with fixed diameter end caps as shown in figure 1 was surrounded by a precision cylindrical form, as shown in figure 2(b), and subjected to internal hydrostatic pressure and axial compressive load. The apparatus used for this process is shown in figure 2. A servo controlled hydraulic compression test machine maintained an axial compressive load slightly less than the internal pressure load on the end caps while allowing the tube to foreshorten as it expanded. The remaining axial tensile load in the tube served to prevent buckling and was maintained by the friction force between the end cap flange and clamp diaphragm. For specimen 7 the precision cylindrical form was modified to have a flat spot of 1.27 cm circumferential width and 12.7 cm length. The resulting imperfection, however, was much greater in width and did not approach flatness.

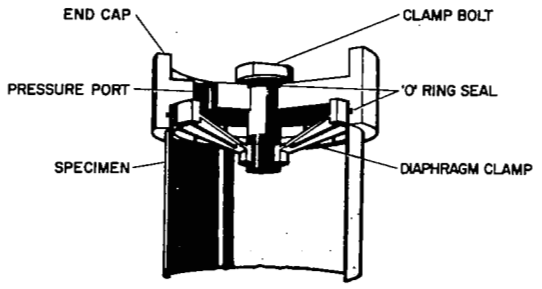

Figure 1.– End fixture assembly used in gripping and sealing cylindrical specimens during expansion process.

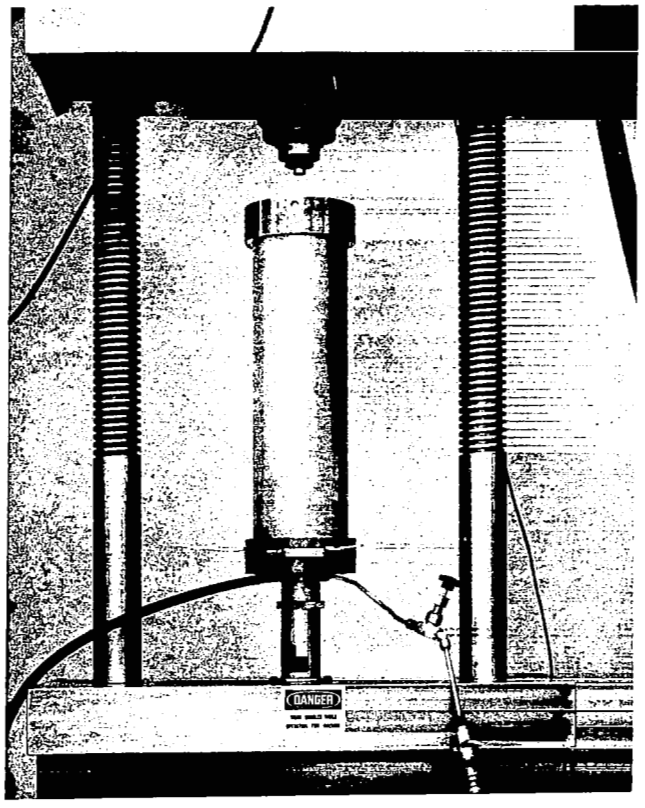

(a) Specimen in test machine prior to expansion.

Figure 2.– Expansion process.

After expanding to 21.6 cm diameter over the full length of the cylindrical form, the tubes were removed from the form and cut to length by a traveling wire electrical discharge cutter. Internal and external clamp rings were then installed at each end of the finished cylinder as shown in figure 3. These pairs of clamp rings were so positioned that the ends of the cylinder extended 0.050 cm beyond them so that only the ends of the cylinder made contact with the loading apparatus. This method was used because it provided a simple means of attaining an unusually high degree of flatness and roundness of the ends of the cylinder, and accommodated minute variations in specimen diameter. The exposed edges were then ground to precision flatness using fine emory paper on a surface plate. The length of the assembled specimens was 19 cm between the inside faces of the end rings.

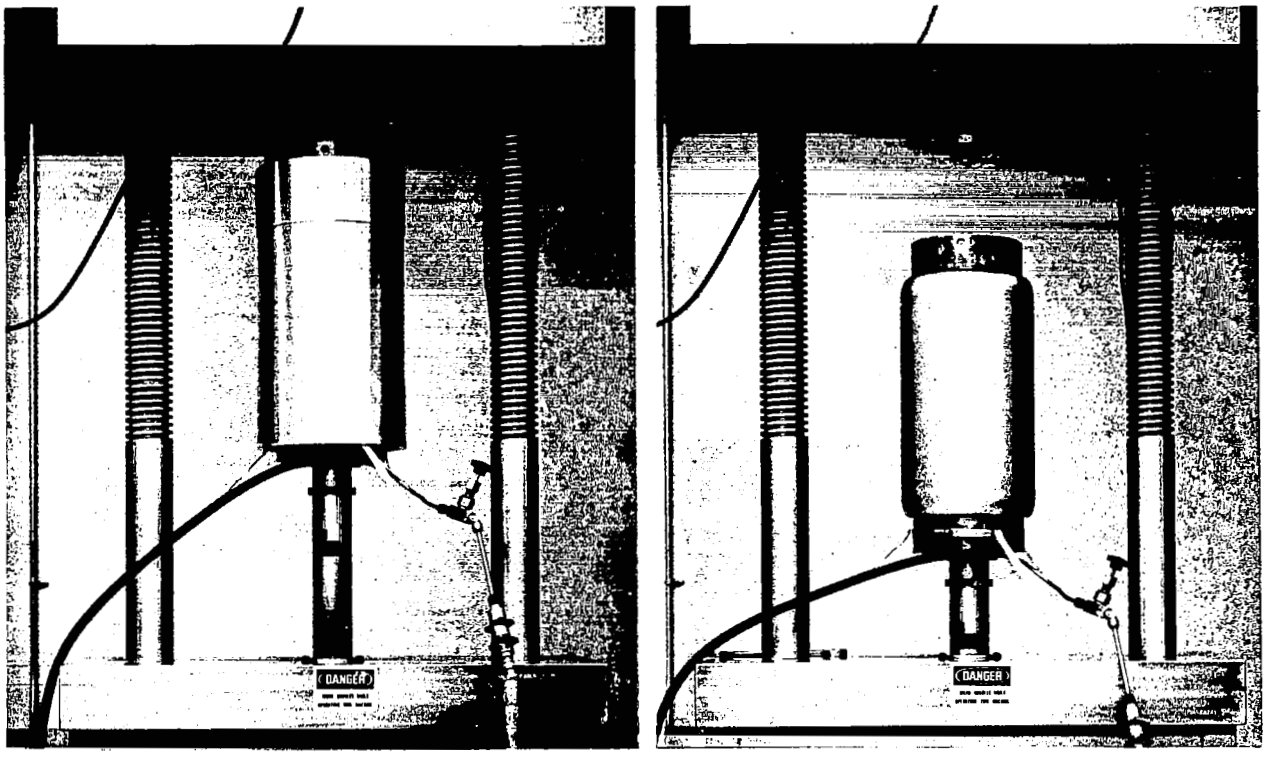

(b) Specimen partially expanded into form. (c) Specimen fully expanded after removal of outer form.

Figure 2.– Concluded.

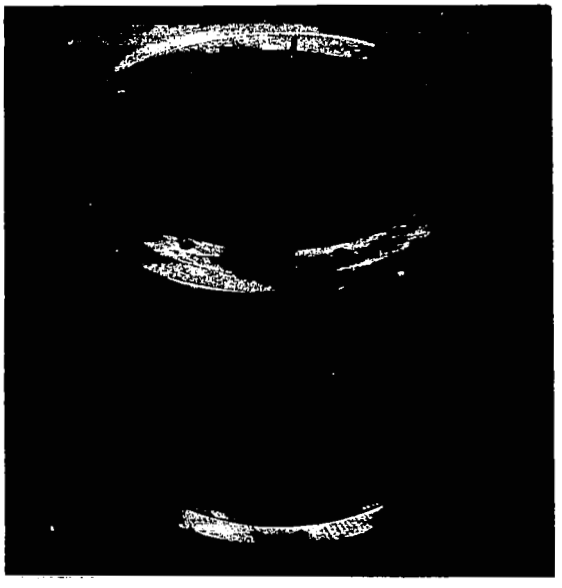

Figure 3.– Completed test specimen.

PHYSICAL PROPERTIES OF SPECIMENS

The plastic expansion process reduced the thickness of the original tubing approximately 16 percent except in the vicinity of the weld seam and in a similar zone diametrically opposite the weld seam. In these zones, which were approximately 1.3 cm wide, the thickness increased gradually to a maximum at the center of the zone which had experienced only a 6-percent thickness reduction. These zones of low ductility are characteristic of the process of welding, weld bead rolling, and annealing used to fabricate the original tubing. The effect of these zones on buckling strength was considered negligible and there was no evidence that buckling was influenced by their presence.

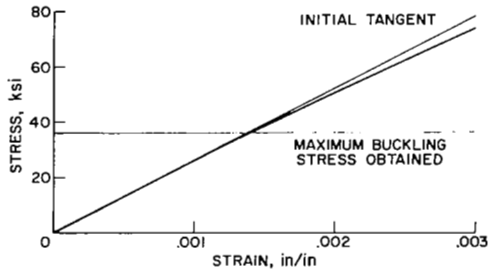

Figure 4.– Stress-strain curve for 304 stainless steel.

No significant difference was observed between axial and circumferential properties. Values of modulus of elasticity varied between 178.0 and 183.0 GN/m^2. An average value of 180.5 GN/m^2 has been taken as representative of the material. A typical stress-strain curve for the material is shown in figure 4.

MEASUREMENT OF INITIAL IMPERFECTIONS

The apparatus shown in figure 5 was used to obtain continuous plots of the radial position of the outer surface of the specimen at 10 positions along its length, beginning 0.635 cm from either

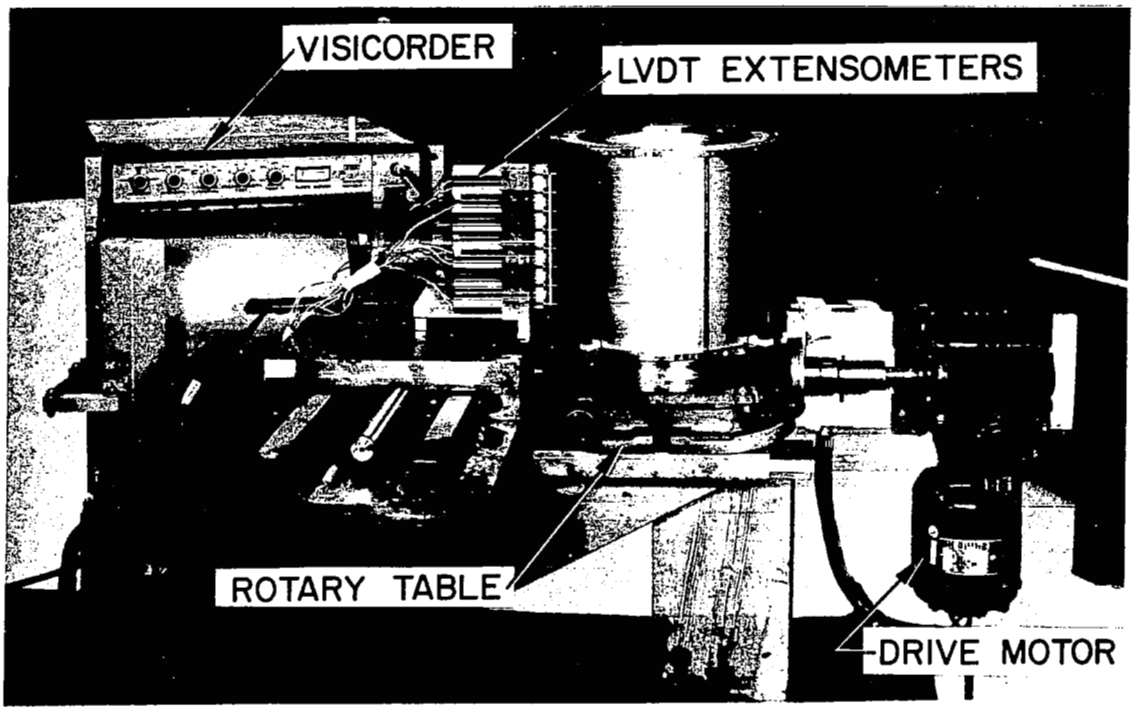

Figure 5.– Apparatus for measuring imperfections.

end. A motor driven rotary table provided constant speed of rotation of the specimen. Eight direct current type LVDT extensometers were used to detect radial motion. The core elements of the extensometers were guided to prevent lateral motion, and were provided with 0.75 mm diameter spherical tips which were kept in contact with the specimen by a light spring load. There was no detectable deformation of the specimen due to the spring load. Although only 8 extensometers were used, data were taken at 10 locations by relocating the bank of extensometers and repeating the measurements. This provided a check on the repeatability of the measurements for the 6 central positions. Data were recorded with an accuracy of ±0.0005 cm on an oscillograph which provided 2.54 cm of motion for 0.0254 cm of deflection.

TEST PROCEDURE

Buckling tests were performed in a 50,000 lb compression testing machine using a rigid lower platen and a spherically seated upper platen, as shown in figure 6. The specimens were subjected to a constant rate of compressive deformation requiring approximately 5 minutes to reach the buckling load. Specimens were observed visually to detect any evidence of local buckling, and continuous plots of load versus machine displacement were made. Care was taken to locate the specimens within ±6 mm of the centerline of loading. As shown in figure 6, loading plates at each end of the specimen distributed the load evenly across the machined grooves in the platens. It is felt that a high degree of load uniformity was achieved by the use of a spherically seated upper platen and by permitting only the ends of the specimens to contact the loading surfaces. The location of the buckled pattern relative to the specimen seam and ends, and the nature of the buckle pattern were noted at the end of each test.

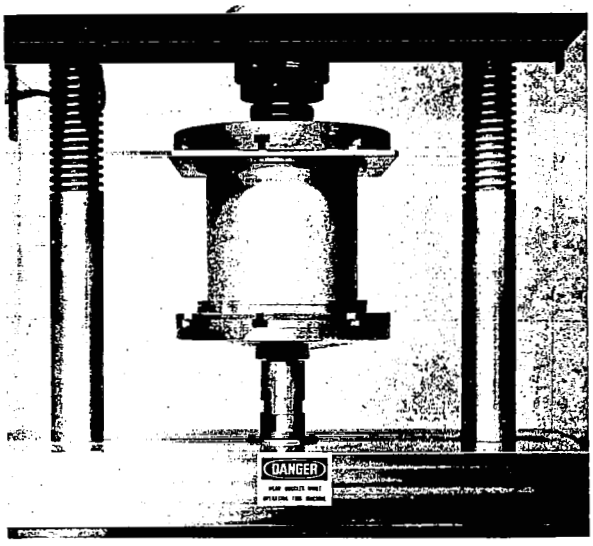

Figure 6.– Buckling test of completed specimen.

TABLE 1.– TEST RESULTS

Specimen	Thickness t, cm	Buckling load P_{CR}, N	P_{CR}/P_{CL}
1	0.03424	53,800	0.66
2	.03363	48,300	.62
3	.03330	52,300	.69
4	.03378	49,000	.62
5	.03373	51,600	.66
6	.03391	56,300	.71
7*	.03391	40,000	.50

*Specimen no. 7 was formed with a deliberate imperfection.

RESULTS

Seven specimens were prepared and tested. Test results are given in table 1, where the value of the classical buckling load has been determined from the expression

$$P_{CL} = 1.212\,\pi E t^2 \qquad (1)$$

in which the coefficient 1.212 was obtained using a value of 0.3 for Poisson's ratio.

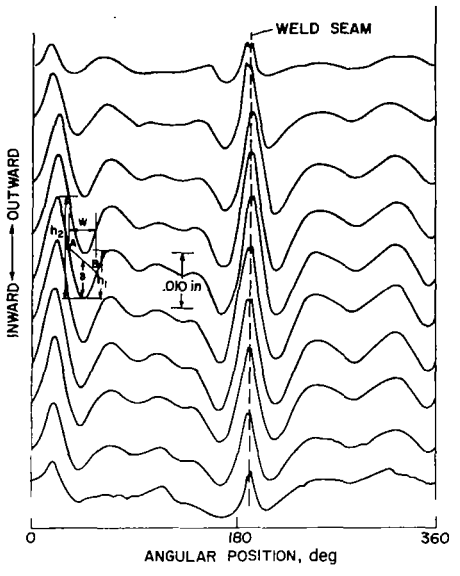

Figure 7.– Imperfection plots for specimen number 3.

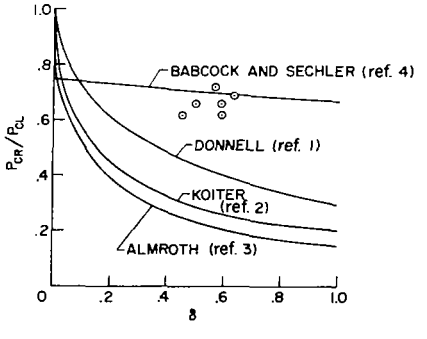

Figure 8.– Buckling load vs. imperfection amplitude.

Plots of geometric imperfections taken around the circumference at 10 lengthwise positions are shown in figure 7 for a typical specimen. The amplitude δ of an inward imperfection peak was taken as half the average peak-to-peak amplitudes, h_1 and h_2, of adjacent peaks as shown in this figure. The width w of the peak was taken as the circumferential distance between the midpoints A and B.

In figure 8, the results of these tests have been superimposed on plots obtained by other investigators showing buckling load as a function of imperfection amplitude. Specimen number 7 is not shown on this plot because its imperfection amplitude lies beyond the range of the abscissa.

DISCUSSION OF RESULTS

As seen in figure 7, the geometric imperfections encountered in this study were characterized by half wavelengths in the direction of the cylinder axis equal to shell length and approximately 7 circumferential waves. All specimens had a maximum amplitude of imperfection at midlength which diminished toward either end, and were strikingly free of any short wavelength variations in the longitudinal direction. This characteristic pattern of imperfections appears to be the result of the process of plastic deformation used in forming the specimens. Figure 8 shows that the buckling loads obtained in this investigation are substantially higher than those predicted theoretically in references 1, 2, and 3, while showing good agreement with loads given by the theory and experiments of reference 4. This latter work, by Babcock and Sechler, however, applies to an axially symmetric inward imperfection whose half wavelength is equal to the shell length and, hence, is free of any circumferential imperfections. The other three works apply to imperfections that are localized in either the longitudinal or the circumferential direction, or both.

It would appear that the specimens tested in this investigation would most logically be evaluated on the basis of their large amplitude, short wavelength, nonaxially symmetric imperfections. As seen from figure 8, however, this kind of evaluation leads to large discrepancies. The good agreement with the prediction from Sechlers work, however, leads to the speculation that such imperfections, which extend to the full length of the shell in the longitudinal direction, are no more severe than an axially symmetric imperfection of the same amplitude.

A closer examination of imperfection data was undertaken to determine whether the variation in buckling load among test specimens showed any correlation with the severity of imperfections. No correlation exists between amplitude of inward imperfections and buckling load as can be seen in figure 8. A definite correlation is obtained, however, between the maximum local curvature reduction created by an inward imperfection peak and buckling load.

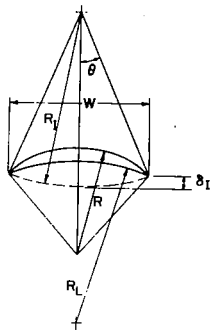

Figure 9.– Relationship between local radius of curvature and imperfection amplitude.

The shape of the curves was studied to determine the curvature decrease caused by an inward half wavelength of the imperfection curve. It was observed that the shape of the most severe inward imperfection waves was very close to a circular arc. This led to the development of a simple expression for the local curvature, R_L, of a cylinder of radius R with such an inward imperfection extending over a width w. If it is assumed that the inward imperfection can be represented by a superimposed circular arc of radius R_I as shown in figure 9, such that δ is the inward displacement due to the imperfection (measured relative to the chord line in fig. 9), then

$$\frac{\delta}{w^2} = \frac{R_I(1 - \cos\theta)}{(2R_I \sin\theta)^2} = \frac{1 - \cos\theta}{4R_I(1 - \cos^2\theta)} = \frac{1}{4R_I(1 + \cos\theta)}$$

Also, for θ sufficiently small that $\cos\theta$ approaches unity, the curvature of the imperfection can be expressed with sufficient accuracy as

$$\frac{1}{R_I} = \frac{8\delta}{w^2} \tag{2}$$

Again, for θ sufficiently small, it can be shown that

$$\frac{1}{R_L} = \frac{1}{R} - \frac{1}{R_I} = \left(1 - \frac{R}{R_I}\right)\frac{1}{R} \tag{3}$$

It can be seen from equation (3) that when $R_I = R$, R_L approaches infinity and the surface is locally flat. Also, when R_I approaches infinity (no imperfection), $R/R_I = 0$ and $1/R_L = 1/R$. Thus we see that the ratio R/R_I is a measure of the curvature decrease due to an inward imperfection wave, and from equation (2),

$$\frac{R}{R_I} = C_I = \frac{8\delta R}{w^2} \tag{4}$$

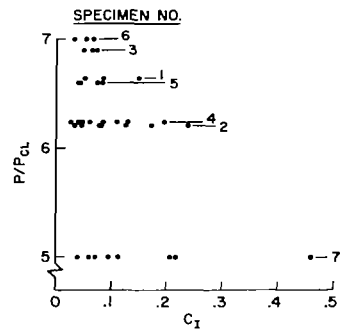

Figure 10.– Buckling load vs. curvature reduction due to imperfections.

In figure 10, the value of C_I for every significant inward imperfection peak on a given specimen is plotted on the same abscissa opposite the corresponding buckling load for that specimen.

The correlation between buckling load of a given shell and the curvature reduction created by its imperfections is clearly shown in this plot by the outermost points for each specimen, which represent the most severe imperfections. This plot is intended to determine in a qualitative way whether the scatter of buckling loads for these tests, which is already quite small, was due primarily to the severity of remaining imperfections, or to variations in load distribution or edge restraint. In view of the correlation indicated, it would appear that variations in these effects were of minor importance in this series of tests.

The relationship indicated in figure 10 between local curvature and buckling load leads to the consideration of a minimum value of buckling load for the case of zero curvature or a flat spot. The buckling load of an axially loaded cylinder containing a flat spot imperfection has been predicted in reference 5 by Reed, and is given by

$$\frac{P(w)}{P_{CL}} = \frac{kRt}{w^2}, \qquad kRt \leq w^2 \tag{5}$$

where k is the coefficient determined by the type of edge constraints assumed for the flat region, and w is the circumferential width of the region. Reed suggests that such a cylinder will buckle at the plate buckling load of the flat spot or the classical buckling load of the cylinder whichever is lower, which implies a minimum or critical width of flat spot. The critical width is given in reference 5 as

$$w_{CR} = 2.4\sqrt{12t} = \sqrt{5.77Rt} \tag{6}$$

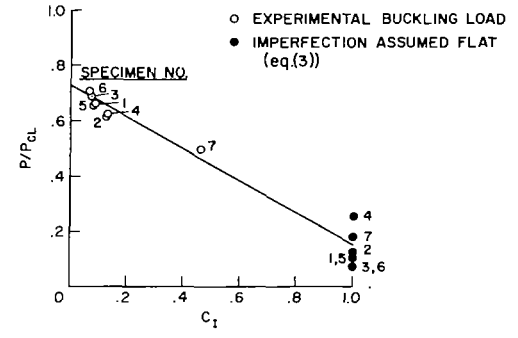

Figure 11.– Comparison of buckling load for "worst" imperfections with "flat spot" buckling loads.

which corresponds to the case of a simply supported plate the size of the flat spot and a value of k = 5.77. For any given inward imperfection peak of width w then, a load can be calculated from equation (5) representing the buckling load corresponding to a flat spot of the same width. Values of "flat spot" buckling load (C_I = 1, solid points), are shown in figure 10 for each specimen, using a value of w in equation (5) corresponding to the most severe inward imperfection judged on the basis of both curvature reduction and w/w_{CR}. The circled points in figure 11 represent these most severe inward imperfections plotted versus their actual curvature reduction.

The maximum value of P/P_{CL} corresponding to a perfect cylinder would appear to be approximately 0.75 if these data were extrapolated. A value ranging from approximately 0.85 to unity would be expected from theory for the boundary condition used in these tests. (See ref. 6.) This discrepancy could not be explained in terms of test procedure and results. It is assumed to be due to the difference between actual test conditions and those assumed in classical theory, such as nonuniform conditions of end restraint and load distribution. Such a discrepancy has been noted by other investigators including Sechler (ref. 4). The straight line plotted in figure 11 was obtained by expressing buckling load as a function of local curvature between the "reduced" buckling load for a perfect cylinder, which does not appear to depend upon imperfections, and the "flat spot" buckling load. The "flat spot" buckling load chosen for this curve was the one obtained from equation (5) using the average of the widths of the most severe imperfection of each specimen. The linear relation for buckling load becomes simply

$$P_B = B\left(1 - \frac{R}{R_I}\right) P_{CL} + \frac{R}{R_I} P_{(w)} \tag{7}$$

where P_B is the actual buckling load, $P_{(w)}$ is the 'flat spot" predicted buckling load, and P_{CL} is the classical buckling load. The factor B accounts for the reduced buckling load observed in experiments for "perfect" cylinders. Combining equations (3), (5), (6), and (7) yields,

$$P_B = \left[B \frac{R}{R_L} + \left(1 - \frac{R}{R_L}\right)\left(\frac{w_{CR}}{w}\right)^2\right] P_{CL} \tag{8}$$

It can be seen in figure 11 that the loads predicted for flat spots fall reasonably well on the straight line obtained from equation (8). This implies that the buckling load of a cylinder is determined by the width and local curvature in the region of the most severe inward imperfection.

It should be noted, however, that equation (8) contains the condition that $w \geq w_{CR}$ as presented in reference 5, which implies that flat spots shorter than w_{CR} do not reduce the buckling load of a cylinder.

CONCLUSION

The buckling loads obtained in this investigation were considerably greater than would be expected in view of the amplitude and shape of their geometric imperfections. The process of hydrostatic expansion used in forming the test specimens results in a unique shape of imperfection characterized by relatively short circumferential waves and longitudinal half wavelengths extending over the full length of the shell. The effect of these imperfections was no more severe than an axisymmetric imperfection of the same maximum amplitude extending over the entire shell length. A relationship was noted between buckling load and the local curvature reduction caused by an inward imperfection which shows some agreement with buckling loads predicted for flat spots.

These results, although based on only seven tests, using simple specimen preparation and testing procedures, lead us to the conclusion that the process of plastic expansion offers an opportunity to produce cylinders of unusually high buckling load at relatively low cost.

Ames Research Center
National Aeronautics and Space Administration
Moffett Field, California, 94035, Dec. 1, 1970,

REFERENCES

1. Donnell, L. H.; and Wan, C. C.: Effect of Imperfections on Buckling of Thin Cylinders and Columns Under Axial Compression. J. Appl. Mech., vol. 17, no. 1, March 1950, pp. 73-83.

2. Koiter, W. T.: The Effect of Axisymmetric Imperfections on the Buckling of Cylinderical Shells Under Axial Compression. Lockheed Missile and Spacecraft Rep. LMSC 6–90–63–86, Aug. 1963.

3. Almroth, B. O.: Influence of Imperfections and Edge Restraint on the Buckling of Axially Compressed Cylinders. NASA CR–432, 1966.

4. Babcock, C. D.; and Sechler, E. E.: The Effect of Initial Imperfections on the Buckling Stress of Cylindrical Shells. NASA TN D–2005, 1963.

5. Reed, Robert E., Jr.: Remarks on Imperfections of Axially Loaded Cylinders. NASA TM X–1552, 1968.

6. Stein, Manuel: Some Recent Advances in the Investigation of Shell Buckling. AIAA J., vol. 6, no. 12, Dec. 1968, pp. 2339–2345. Also in AIAA Paper 68–103, Jan. 1968.

NASA-Langley, 1971 —— 32 A–3733